

1 **Upwelling characteristics in the Gulf of Finland (Baltic Sea) as revealed by Ferrybox**
2 **measurements in 2007-2013**

3

4 Villu Kikas, Urmas Lips

5

6 Marine Systems Institute at Tallinn University of Technology

7 Akadeemia tee 15a, 12618 Tallinn, Estonia

8 Tel: +3726204315, Fax: +3726204301

9 e-mail: villu.kikas@msi.ttu.ee

10

11 **Abstract.** Ferrybox measurements are carried out between Tallinn and Helsinki in the Gulf of
12 Finland (Baltic Sea) on a regular basis since 1997. The system measures autonomously water
13 temperature, salinity, chlorophyll *a* fluorescence and turbidity and takes water samples for
14 further analyses at a predefined time interval. We aimed to show how the Ferrybox technology
15 could be used to study the coastal upwelling events in the Gulf of Finland. Based on the
16 introduced upwelling index and related criterion, 33 coastal upwelling events were identified in
17 May-September 2007-2013. The number of events, as well as the frequency of their occurrence
18 and intensity expressed as a sum of daily average temperature deviations in the 20-km wide
19 coastal area, were almost equal near the northern and southern coast. Nevertheless, the wind
20 impulse, which was needed to generate upwelling events of similar intensity, differed between
21 the northern and southern coastal area. It is suggested that the general thermohaline structure
22 adapted to the prevailing forcing and the estuarine character of the basin weaken the upwelling
23 created by the westerly-southwesterly (up-estuary) winds and strengthen the upwelling created
24 by the easterly-northeasterly (down-estuary) winds. Two types of upwelling events were
25 identified – one characterized by a strong temperature front and the other revealing gradual
26 decrease of temperature from the open sea to the coastal area with maximum temperature
27 deviation close to the shore.

28

29 **Keywords:** Ferrybox, coastal upwelling, upwelling index, cumulative wind stress, Gulf of
30 Finland

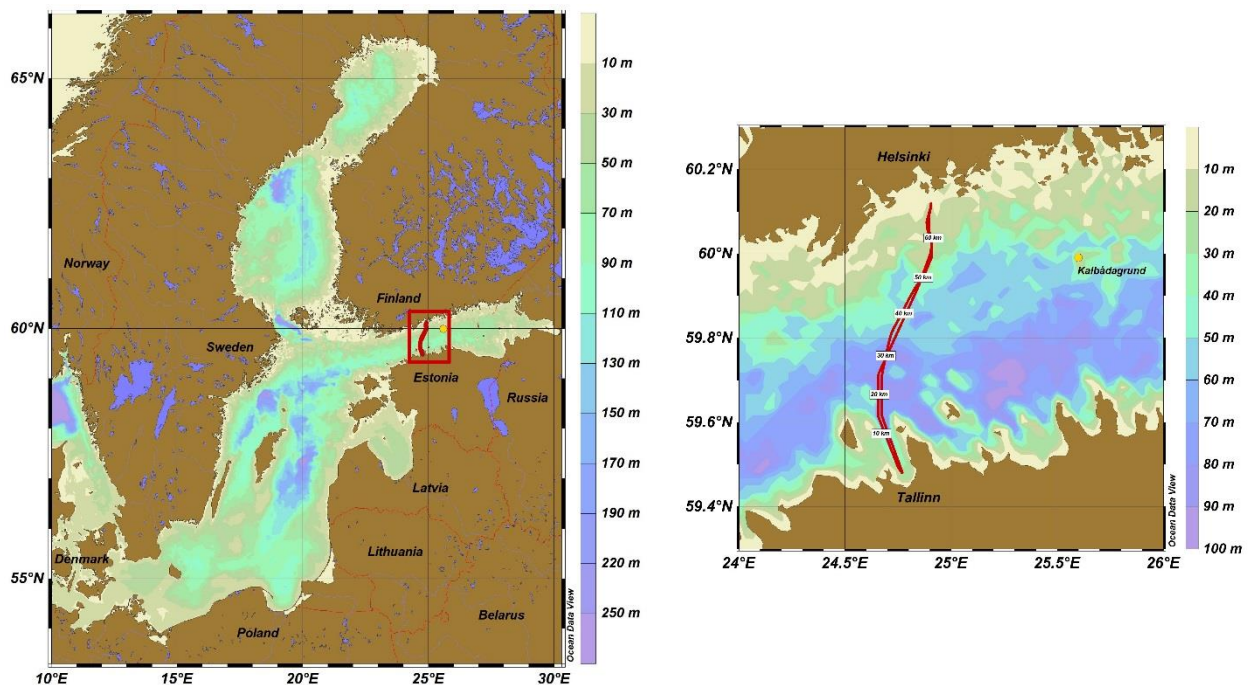
31

33 **1. INTRODUCTION**

34

35 Unattended monitoring of marine environment using ships of opportunity has been implemented
36 in many regions of the World Ocean (e.g. Paerl et al., 2009; Hardman-Mountford et al., 2008)
37 including the Baltic Sea and the Gulf of Finland (Rantajarvi, 2003). The measurement systems
38 installed on board commercial ferries or other ships are called “Ferryboxes” and they consist of
39 various sensors, devices creating water flow through the sensors and software packages
40 controlling the system and managing the data. The commonly used Ferryboxes measure
41 temperature, salinity, and chlorophyll *a* fluorescence in the seawater pumped through the system
42 from the surface layer along the ship track. First trials of using ships of opportunity for
43 environmental monitoring in the Gulf of Finland were made by Estonian and Finnish scientists
44 between Tallinn and Helsinki in 1990-1991 (Rantajarvi, 2003). Regular Ferrybox measurements
45 along this route were started in 1997 while the longest data series of Ferrybox measurements
46 (since 1993) is available along the ferry route Helsinki-Travemünde (Petersen, 2014).

47



48 **Figure 1. Map of the Baltic Sea (a) and the study area (b) with the Ferrybox transect and Kalbadagrund meteorological station.**

49

50 The Gulf of Finland (GoF) lies in the northeastern part of the Baltic Sea (Fig. 1). It is an
51 elongated basin with a length of about 400 km and a maximum width of 135 km (Alenius et al.,
52 1998). The long-term residual circulation in the surface layer of the gulf is characterized by a
53 relatively low speed and by a cyclonic pattern. The saltier water of the northern Baltic Proper
54 flows into the gulf along the Estonian (southern) coast and the gulf water, which is less saline
55 due to the large freshwater inflow at the eastern end of the gulf (the Neva River), flows out along
56 the Finnish (northern) coast. The circulation is more complex at time scales from days to weeks
57 mainly due to the variable wind forcing. A variety of mesoscale processes/features (fronts,
58 eddies, upwelling/downwelling), which significantly affect the biological production, retention,
59 and transport, have been observed in the Gulf of Finland (e.g. Talpsepp et al., 1994; Pavelson et
60 al., 1997; Lips et al., 2009).

61

62 The vertical stratification in the gulf is characterized by a quasi-permanent halocline at the
63 depths of 60-80 m, and a seasonal thermocline, which forms in spring-summer at the depths of
64 10-20 m (e.g. Liblik and Lips, 2011). While high concentrations of dissolved inorganic nitrogen
65 (DIN) and phosphorus (DIP) are observed in winter, the concentrations of DIN and DIP are
66 usually below the detection limit in summer in the upper mixed layer but still high just below the
67 seasonal thermocline. In general, the most prominent features of the seasonal dynamics of
68 phytoplankton in the Gulf of Finland are the spring bloom in April-May dominated by
69 dinoflagellates/diatoms and the late summer bloom in July (or late June to mid-August)
70 dominated by cyanobacteria (Kononen et al., 1996). However, the variations in bloom intensities
71 and their spatial distributions are very high over the years and within the season that is often
72 related to the physical forcing and especially to the mesoscale processes, including upwelling
73 events (Lips and Lips, 2008; Vahtera et al., 2005).

74

75 Dynamics and characteristics of upwelling events have been studied in the Gulf of Finland based
76 on in-situ measurements (e.g. Haapala, 1994), remote sensing (e.g. Uiboupin and Laanemets,
77 2009) and modeling (e.g. Myrberg and Andrejev, 2003). Most prominent upwelling events that
78 were captured by measurements are an event along the northern coast in July 1999 (Vahtera et
79 al., 2005) and an event along the southern coast in August 2006 (Lips et al., 2009). The
80 following characteristic features of upwelling events in the Gulf of Finland are suggested:

81

82 1) the Finnish coastal sea in the north-western GoF is one of the main upwelling areas in the
83 Baltic Sea (Myrberg and Andrejev, 2003) where upwelling frequency in May-September
84 1990-2009 has been up to 15% (Lehmann et al., 2012); almost the same upwelling
85 frequency is suggested by the latter authors for the central GoF along the Estonian
86 (southern) coast;

87 2) mean upwelling area detected on the basis of 147 maps during the period of 2000-2009
88 was 5642 km² (19% of the GoF surface area) along the northern coast and 3917 km²
89 (13% of the GoF surface area) along the southern coast (Uiboupin and Laanemets, 2015),
90 while the largest area covered by the upwelling water was identified as 12140 km² (data
91 from 2000-2006; Uiboupin and Laanemets, 2009); the authors' estimate of the mean
92 cross-shore extent of upwelling area was 20-30 km off the northern coast and varied
93 between 7 and 20 km off the southern coast;

94 3) the intensity of upwelling events depends on the values of cumulative upwelling-
95 favorable wind stress and strength of vertical stratification; Haapala (1994) suggested that
96 at least 60 h long wind event has to exist to create an upwelling event; based on the wind
97 data analysis from 2000-2005 and taking the threshold value for cumulative wind stress
98 of 0.1 N m⁻² d, on average, about 2 upwelling events should appear off the southern coast
99 and 4 events off the northern coast (Uiboupin and Laanemets, 2009);

100 4) it is suggested that the difference in topography off the southern and northern coast of the
101 GoF results in differing upwelling dynamics along the opposite coasts – in case of similar
102 wind stress (but in opposite directions) the transport of waters from deeper layers starts
103 earlier and is larger along the southern coast (Väli et al., 2011).

104

105 The motivation of the present paper is to show how the Ferrybox technology can be used to
106 study mesoscale processes, especially coastal upwelling events in the Gulf of Finland. We
107 describe the approach, its advantages and limits, and present statistical characteristics of
108 upwelling events on the basis of data collected in 2007-2013. The main aims are to relate the
109 observed variability and dynamics of upwelling events to the atmospheric forcing, to reveal the
110 differences in upwelling behavior in the northern and southern coastal areas, and to suggest an

111 alternative physical explanation of the found differences by taking into account the prevailing
112 forcing and estuarine character of the basin.

113

114 **2. THE MEASUREMENT SYSTEM AND METHODS**

115

116 **2.1. Ferrybox system**

117

118 Temperature (T), salinity (S), chlorophyll *a* fluorescence and turbidity data and water samples
119 for nutrients and phytoplankton chlorophyll *a* (Chl *a*), species composition and biomass analyses
120 are collected unattended on passenger ferries, traveling between Tallinn and Helsinki (Fig. 1)
121 since 1997. Due to the internal arrangements of the ferry company Tallink Silja and its
122 predecessors, several ships were used as the platforms for Ferrybox measurements, which also
123 differ regarding water intake features. A flow-through system from 4H-Jena, Germany with the
124 water intake attached to the sea chest of the ferry has been in use since 2006. The water enters
125 the sea chest through a grating with a total surface area of 0.84 m² located at about 4 m depth
126 below the waterline. The water flow from the sea chest into the system is forced by the
127 hydrostatic pressure since the Ferrybox is located on the lower deck about 3 meters below the
128 waterline. To restrict larger particles to get into the measurement system a mud filter (pore size 1
129 mm) is used close to the water intake. Before the sensors, a debubbler is installed to avoid air
130 bubbles to affect the measurements of conductivity, turbidity and Chl *a* fluorescence. The flow
131 rate through the sensors is stabilized by an internal pump, which is controlled by a pressure
132 sensor in the system. Water samples are taken by a sampling device (Hach Sigma 900 MAX)
133 whereas the water is pumped from the debubbler into the bottles using an internal pump of the
134 water sampler.

135

136 For temperature measurements, a PT100 temperature sensor is used that is installed close to the
137 water intake to diminish the effect of warming of water while flowing through the tubes onboard.
138 The sensor has a measuring range from -2 to +40 °C and accuracy of ±0.1% of the range, thus
139 0.04 °C. For salinity measurements an FSI Excell thermosalinograph (temperature and
140 conductivity meter) and for Chl *a* fluorescence and turbidity measurements a SCUFA
141 submersible fluorometer (Turner Designs) with a flow-through cap is used. The system starts the

142 measurements and data recording when the ferry is away from the harbor more than a predefined
143 distance of 0.7 nautical miles (controlled by a GPS device in the system) and stops when it is
144 closer than this distance to avoid sediments getting into the system. The data are recorded during
145 every crossing (twice a day) every 20 seconds that corresponds to a horizontal resolution of
146 approximately 160 m.

147

148 **2.2. Quality assurance and pre-processing of data**

149

150 The sensors have been calibrated at the factory before the installation and if necessary sent for an
151 additional laboratory calibration. Since the system contains two temperature sensors, the
152 performance of them is routinely followed by a comparison of data acquired from the sensors.
153 The quality of thermosalinograph data is guaranteed by taking a series of water samples (14-17
154 samples) and analyzing them using a high-precision salinometer AUTOSAL 2-4 times a year.
155 The analyses have shown, that a correction of 0.08 (units in Practical Salinity Scale; the value
156 has been stable over the years) must be added to the recorded salinity. While the raw salinity is
157 recorded in units according to the Practical Salinity Scale 1978, the results on salinity
158 distribution and variability are given later in this paper in g kg^{-1} (Sections 3 and 4). Particular
159 care is taken to calibrate the SCUFA fluorometer; however, since we do not use the fluorometer
160 data in this study the used routine is not described here.

161

162 The data acquired by the Ferrybox system recorded with a time step of 20 s are stored in an
163 onboard terminal. To synchronize the measurements performed by the sensors having different
164 sampling frequencies and GPS, the acquired data within every 19 s interval are averaged and
165 recorded as measurements at every 20th second. The data are automatically delivered to the on-
166 shore FTP-server once a day when the ferry is in the harbor using a GSM connection. The
167 performance of the system is validated by the control parameters, such as the flow rate and
168 pressure in the system, and the data are checked for unrealistic values against the criteria set for
169 every parameter on the basis of known natural variation of them in the Gulf of Finland.

170

171 One of the procedures, which has to be carried out when using the Ferrybox data, is the shifting
172 of data points to the actual positions of the water intake. The problem arises since the coordinates

173 attached to a data record correspond to the location of the ferry at the time of measurement, but
174 the water is taken in earlier at a different position. Since various systems of water intake are
175 applied, this procedure is unique for each combination of a Ferrybox and a ferry. As described
176 above, in our design the seawater enters first a relatively large sea chest and the flushing through
177 time of it is unknown. While the water flows through the sea chest and into the tubes and
178 debubbler with a flow rate of 12-15 l min⁻¹, the ferry moves on at an average speed of 16 knots.
179 We solved the problem of position correction taking into account the advantage of having two
180 crossings a day.

181
182 Analysis of data from forth and backward journeys allowed us to introduce a position correction
183 procedure – the best result is achieved by shifting the measured data points against the GPS time
184 for 3-4 minutes depending on the ferry and exact intake installation. This relatively long period is
185 obviously related to the water exchange in the sea chest. Due to an almost constant cruising
186 speed of the ferry outside the harbor areas, the applied procedure gives acceptable results. The
187 comparison of data from Tallinn to Helsinki and back from Helsinki to Tallinn obtained on the
188 same day is one of the used quality assurance procedures – the profiles containing unexpected
189 deviations are marked by a quality flag indicating a possible quality problem.

190 191 **2.3. Data and calculation methods**

192
193 Temperature and salinity data collected along the ferry line Tallinn-Helsinki from May to
194 September in 2007-2013 are used for analysis purposes. In 2008, the system on board the
195 passenger ferry “Galaxy” was in use until 13 July and the measurements started again on 13
196 August when the system was installed on board the ferry “Baltic Princess”. However, due to
197 some technical problems, the regular measurements were successful from 2 September 2008. A
198 failure of the system occurred late August 2012 and, therefore, the data are not available from 29
199 August until the end of September 2012. In early 2013, the next ferry (“Silja Europa”) came to
200 this line and the system was moved again causing a break in the measurements until 15 July
201 2013. The number of crossings with the full data coverage is given in Table 1. Four years –
202 2007, 2009, 2010 and 2011 – were the years with almost complete data coverage while most of
203 the data were not available in the second half of July and August 2008, in September 2012 and in

204 May, June and the first half of July 2013. Thus, the data from all months from May to September
 205 were analyzed at least from six years in 2007-2013.

206
 207 Collected raw data were preliminarily processed, including shifting of measurements as
 208 described in Section 2.2, quality checked and stored in the database. This data set was used to
 209 draw the maps of temporal variations of horizontal distributions of T and S for all studied years
 210 (Fig. 2). A step (cell width) of 0.5 km along the south-north oriented line was used to transform
 211 the data set from the matrix with a constant time step into the matrix with a constant spatial
 212 resolution. The fixed south-north orientation was applied to eliminate the influence of
 213 differences in orientation of the ship track in the southern, central and northern parts of the route
 214 (see Fig. 1) and of possible deviations from the ordinary route. As a result, the extent of the
 215 upwelling area is presented below in the south-north direction, and a coefficient has to be applied
 216 to convert these values to the upwelling extent in the cross-shore direction (as the cosine of the
 217 angle between the south-north direction and a perpendicular line to the shore – approximately 20
 218 degrees).

219
 220 An upwelling index was introduced in the coastal area off the southern coast (UI_S) and off the
 221 northern coast (UI_N). For each crossing, the average water temperature and horizontal profile of
 222 temperature deviations from the average were found. The upwelling index was calculated as a
 223 sum of negative temperature deviations in the 20-km coastal areas as:

$$224 \quad UI_S = \sum_{\Delta T_i < 0}^{i=1 \dots 40} |\Delta T_i| \quad \text{and} \quad UI_N = \sum_{\Delta T_i < 0}^{i=101 \dots 140} |\Delta T_i| \quad (1)$$

225 where ΔT_i is the temperature deviation at 0.5-km cell i from the average temperature of the
 226 crossing. The width of 20 km was selected on the basis of the analysis of all available
 227 temperature data from Tallinn-Helsinki ferry line in 2007-2013 (see Section 3.1 for details). The
 228 daily indexes were obtained by averaging the two upwelling indexes from a single day (from
 229 forth and backward journey of the ferry). The cumulative upwelling index (CUI) can be
 230 calculated by summing up upwelling index values for certain periods. The obtained CUI values
 231 were divided by 40, which is the number of data cells in the 20-km wide coastal area, to keep the
 232 meaning of CUI as the sum of average negative temperature deviations, having a unit of [$^{\circ}\text{C}$
 233 day]:

$$234 \quad CUI_S(n1 \dots n2) = \sum_{j=n1}^{j=n2} \left(\frac{1}{40} UI_{Sj} \right) \quad \text{and} \quad CUI_N(n1 \dots n2) = \sum_{j=n1}^{j=n2} \left(\frac{1}{40} UI_{Nj} \right) \quad (2)$$

235

236 where $n1$ and $n2$ are the start and the end day number of the selected period, for which the
237 cumulative upwelling index is calculated, and UI_{Sj} and UI_{Nj} are the upwelling indexes at day j off
238 the southern and northern coast, respectively. This approach of the *CUI* calculation is similar to
239 those used previously in the studies of upwelling events and their influence on the phytoplankton
240 dynamics in the Gulf of Finland (see e.g. Lips and Lips, 2008; Myrberg et al., 2008).

241

242 An upwelling event can be characterized by the cumulative upwelling index whereas the first and
243 the last day of the event can be defined as the start and end of the period when the upwelling
244 index (UI_N or UI_S) exceeded a certain threshold value. We have defined this threshold value as
245 40 °C, which corresponds e.g. to a 20-km wide upwelling with an average negative temperature
246 deviation of 1 °C. This choice is explained in more detail in Section 3.2.

247

248 Wind data were obtained from the HIRLAM (High-Resolution Limited Area Model) version of
249 the Estonian Meteorological and Hydrological Institute with the spatial resolution of 11 km and
250 the time interval of 3 h (Väli, 2011; Männik and Merilain, 2007). Model data point close to
251 Kalbådagrund, where also a meteorological weather station is located (Finnish Meteorological
252 Institute), was chosen to represent the wind conditions in the study area. The data from
253 Kalbådagrund weather station or the closest HIRLAM model point have also been used in the
254 earlier studies of coastal upwellings in the Gulf of Finland (Lips et al., 2008a; Uiboupin and
255 Laanemets, 2009). According to Keevallik and Soomere (2010), the HIRLAM output matches
256 well with the observations at Kalbådagrund (the wind is measured at 32 m), although the
257 modeled wind direction (at 10 m height) is turned by 20° counter-clockwise from the measured
258 wind direction.

259

260 Wind stress (in N m^{-2}) is calculated for the wind component along the axis of the Gulf of
261 Finland, which corresponds to the direction turned by 70 degrees clockwise from the north
262 direction, as:

$$263 \quad \tau_{70} = C_D \rho_a |U| U_{70} \quad (3)$$

264 where U is the wind speed (in m s^{-1}), U_{70} is its component in the along-gulf direction, C_D is the
265 drag coefficient (a value of $1.2 \cdot 10^{-3}$ was chosen in the present study), and ρ_a is the air density

266 (1.2 kg m⁻³). Accordingly, positive values of the wind stress should initiate southward Ekman
267 transport in the surface layer and vice versa. The cumulative wind stress (in N m⁻² day) was
268 calculated based on daily averages of wind stress. If the cumulative wind stress is large enough,
269 upwelling events occur along the northern coast in case of the positive wind stress and along the
270 southern coast in case of the negative wind stress.

271

272 **3. RESULTS**

273

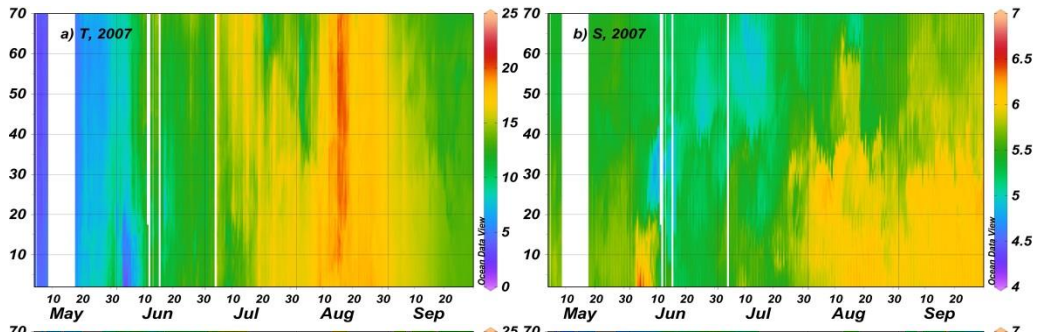
274 **3.1 General variability and distribution patterns**

275

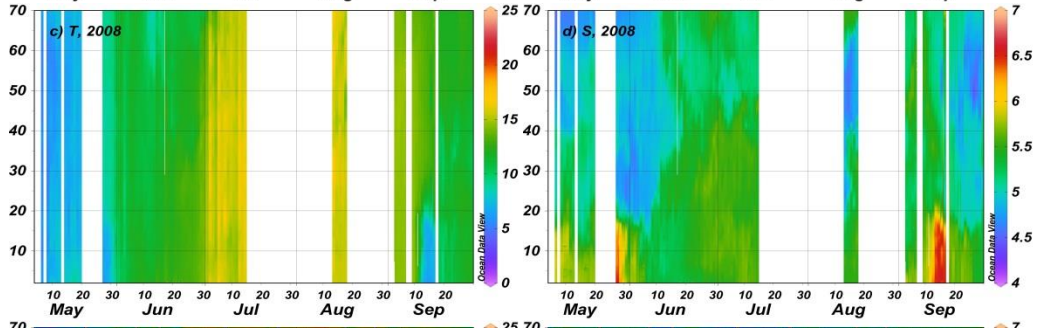
276 The typical seasonal trend of the surface layer temperature in the Gulf of Finland is characterized
277 by temperature about 5 °C at the beginning of May, a maximum > 20 °C in late July – early
278 August and a drop below 15 °C in late September. Within the analyzed years 2007-2013, the
279 surface layer temperature was the highest in summer 2010 (Fig. 2) when the period with the
280 average along-transect temperature > 20 °C was 35 days. On the background of seasonal trend
281 and simultaneous shorter-term increases or decreases of temperature over the whole study
282 transect, the periods with distinctly lower temperature were observed off the northern or southern
283 shore. Such situations are related to the coastal upwelling events – their characteristic time scale
284 was several days to 1-2 weeks, and they extended towards the open sea by 15-20 km (Fig. 2).

285

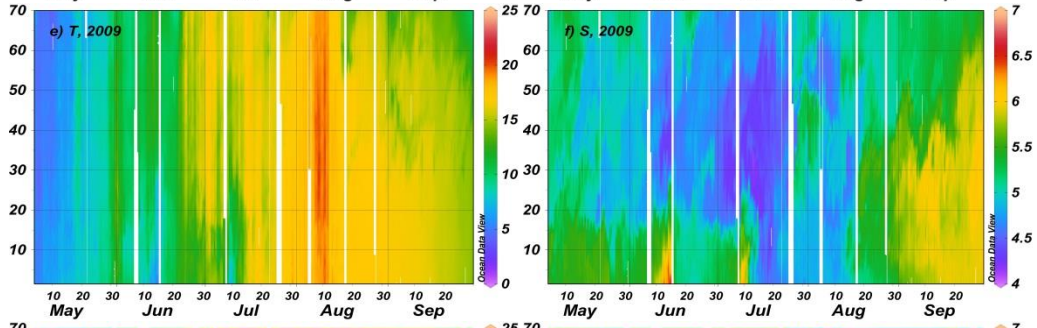
286



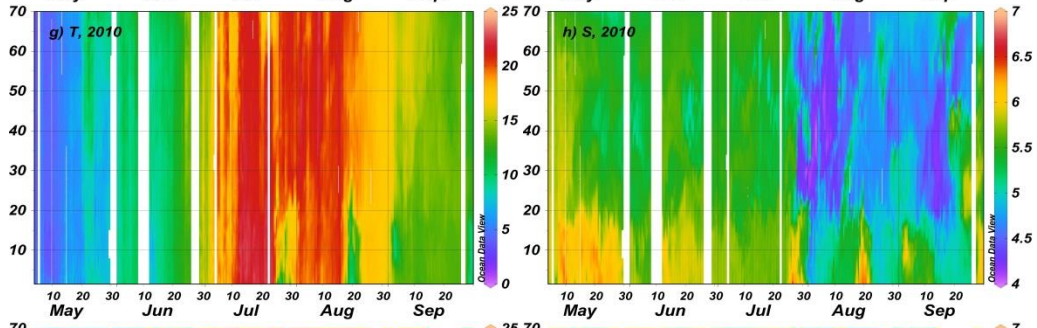
287



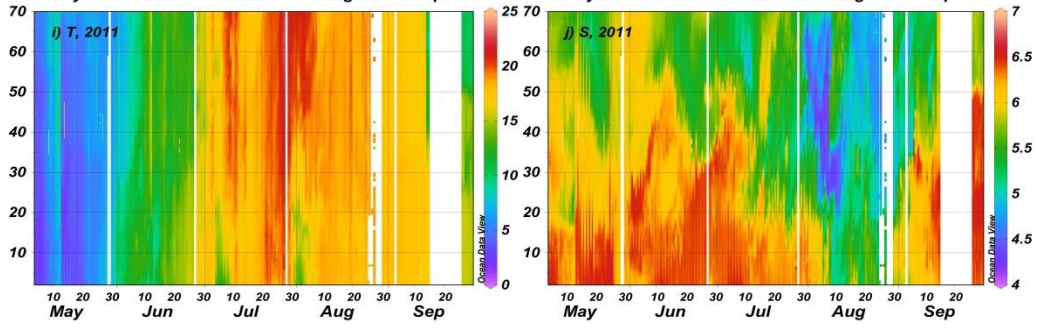
288



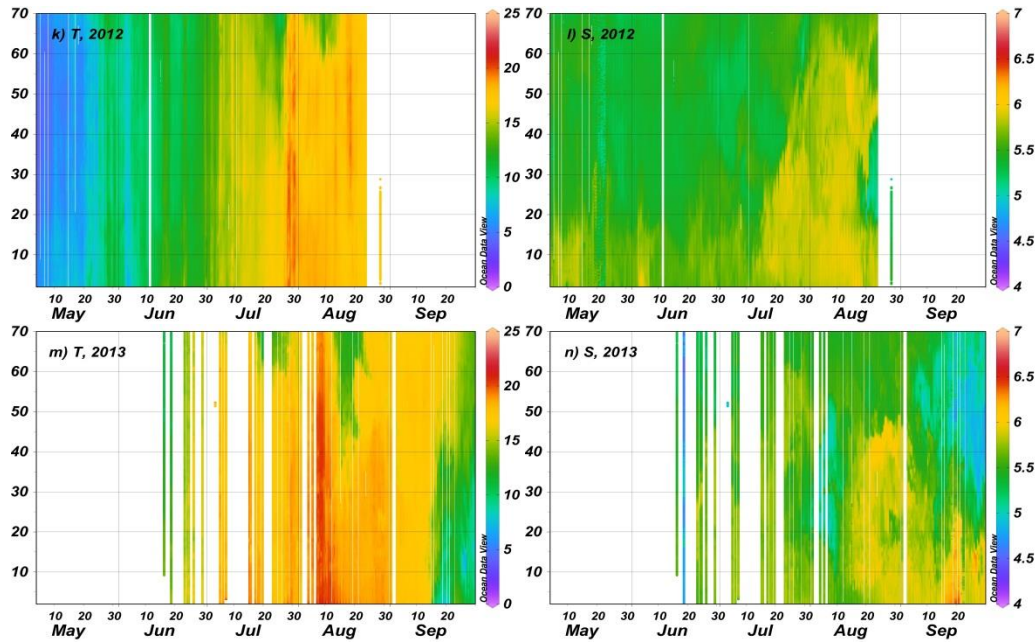
289



290



291

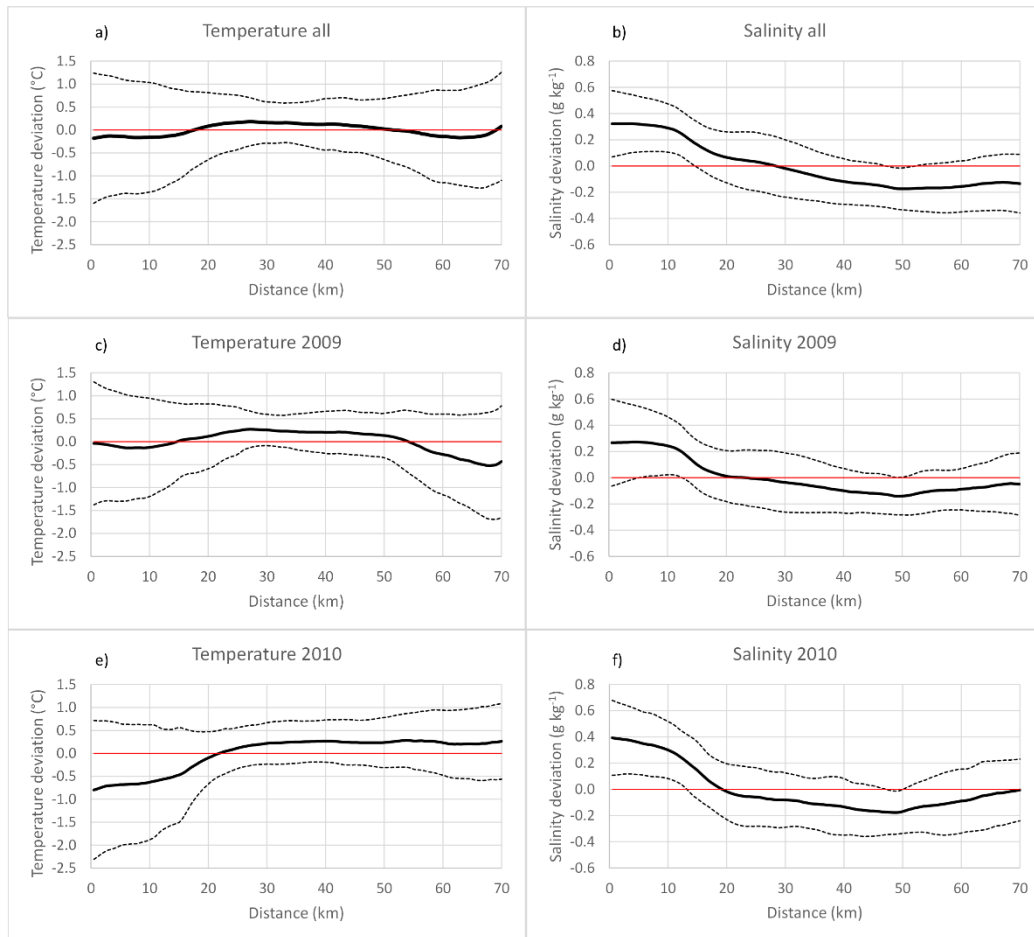


292

293 **Figure 2. Temporal changes in temperature (in °C) and salinity (in g kg^{-1}) distributions between Tallinn and Helsinki from 1 May to 30**
 294 **September in 2007 (a, b), 2008 (c, d), 2009, (e, f), 2010 (g, h), 2011 (i, j), 2012 (k, l) and 2013 (m, n); y-axis shows the distance from the Tallinn**
 295 **Bay (latitude 59.48 N) in km along the meridional transect.**

296

297 Inter-annual variations of the surface layer salinity in 2007-2013 were high with the highest
 298 salinity in 2011 and the lowest in 2009. The surface layer salinity exceeded 6.5 g kg^{-1} for a
 299 longer period only in 2011 in the southern half of the study transect (Fig. 2j) and for shorter
 300 periods of several days in case of coastal upwelling events off the southern shore (e.g. Figs. 2b
 301 and 2d). Note that in the case of coastal upwelling events seen in the temperature distributions
 302 off the northern coast, a simultaneous increase in salinity was not well visible. As a rule, the
 303 surface layer salinity was higher near the southern coast than that near the northern coast.
 304 However, often the lowest salinity was measured in the middle of the transect – it means in the
 305 open sea areas (e.g. Figs. 2f and 2h). Seasonal trend of salinity differed between the studied years
 306 remarkably. While usually, the lowest surface layer salinity was observed in June-July, in 2008,
 307 the salinity was the lowest in May, and in 2010 and 2011, it was the lowest in August.



308

309

310

311

312

313

Figure 3. Distributions of temperature (in °C) and salinity (in g kg^{-1}) deviations from the transect mean value along the ferry route Tallinn-Helsinki for all measurements in May-September 2007-2013 (a, b), 2009 (c, d) and 2010 (e, f). Mean values for each 0.5-km cell (solid curves) and plus/minus RMSE (dashed curves) are shown; x-axis indicates the distance from the Tallinn Bay (latitude 59.48 N) in km along the meridional transect.

314

315

316

317

318

319

320

321

322

323

The average temperature and salinity deviations in May-September each year and for the entire study period, as well as their root mean square errors (RMSE), were calculated in each 0.5-km cell. On average, the temperature deviations were close to zero along the entire study transect (Fig. 3a) – the absolute values of average deviation were six times less than estimated RMSE of temperature. Nevertheless, the surface layer temperature was slightly warmer in the open Gulf of Finland than in approximately 20-km wide coastal areas (Fig. 3a). This result could be related to the coastal upwelling events. For instance, in 2009, when coastal upwelling events were observed off the both coasts, the average temperature deviations were negative near the both coasts (Fig. 3c). In 2010, when upwelling events occurred mostly off the southern coast, the

324 negative values of average temperature deviations were detected only in the southern part of the
325 transect (Fig. 3e).

326
327 It is remarkable that, on average, the variability of temperature deviations was much higher near
328 the coasts than in the central part of the study transect (Fig. 3a). In the case of upwelling events
329 off the southern coast and their absence off the northern coast (in 2010), this high variability of
330 temperature was concentrated only in the 20-km wide coastal area off the southern shore (Fig.
331 3e). Since the area of the high variability of temperature, which mostly could be related to the
332 upwelling activity, extended about 20 km from the shores, we estimated the intensity of
333 upwelling events based on data from these 20-km wide coastal zones.

334
335 The average distribution of the surface layer salinity along the transect was characterized by
336 higher salinity values in the southern gulf and lower values in the northern gulf (Fig. 3b). The
337 salinity deviations were positive in the 28-km wide area off the southern coast (with clearly
338 higher salinity in the first 10 km) and negative along the rest of the study transect. However, the
339 minimum of the surface layer salinity was observed at about 20 km from the northern shore (or
340 at a distance of 50 km from the southern end of the study transect) almost in every year (Fig. 3b,
341 d, and f). The only exception was the year 2007 when the lowest salinity was observed on
342 average in the cell closest to the northern shore. The low salinity water at the distance of 50 km
343 indicates that, in summer, the outflow of the less saline Gulf of Finland surface waters occurs
344 mostly in the northern part of the open gulf. The variability of the surface layer salinity did not
345 differ between the coastal and open sea areas as much as the variability of the surface layer
346 temperature. One can recognize slightly higher variability (RMSE) of the surface layer salinity in
347 the coastal areas and the southern part of the open gulf at a distance of 20-30 km.

348

349 **3.2 Upwelling characteristics**

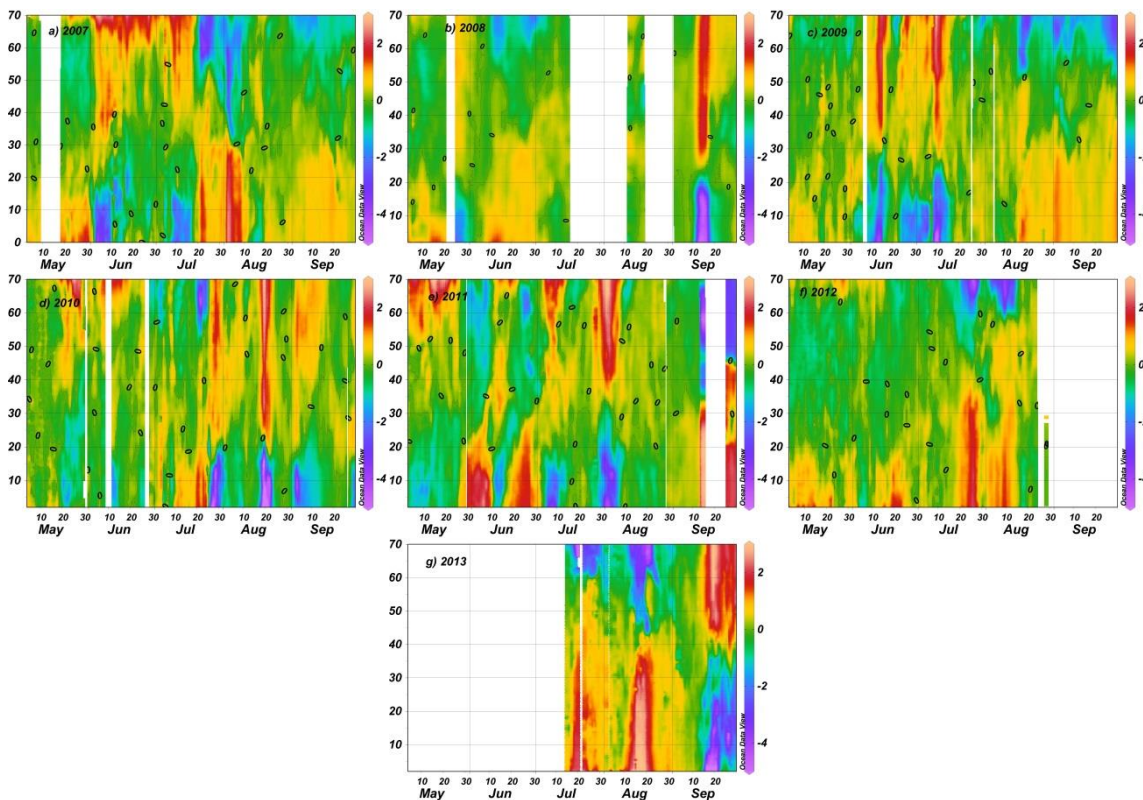
350

351 As it is seen on the maps of temperature deviations (Fig. 4), the years 2007 and 2009 had a
352 similar pattern – the upwelling events occurred off the southern coast in the first half of the
353 season and off the northern coast in the second half. In 2008, upwelling events were observed
354 near the southern coast in May and September, and they appeared near the northern coast in

355 June. The year 2010 was an exceptional year when the upwelling events occurred mostly along
 356 the southern coast. It was exceptional also because the sea surface temperature outside the
 357 upwelling waters was the highest among the studied summers. A sequence of consecutive
 358 upwelling events near the northern and southern coast was observed in 2011. Upwelling events
 359 occurred mostly off the northern coast in 2012 and 2013.

360

361



362

363

364 **Figure 4. Temporal changes in spatial distributions of temperature deviations (in °C) from the daily transect mean value between Tallinn and**
 365 **Helsinki from 1 May to 30 September in 2007 (a), 2008 (b), 2009, (c), 2010 e), 2011 (f), 2012 (g) and 2013 (h); y-axis shows the distance from**
 366 **the Tallinn Bay (latitude 59.48 N) in km along the meridional transect.**

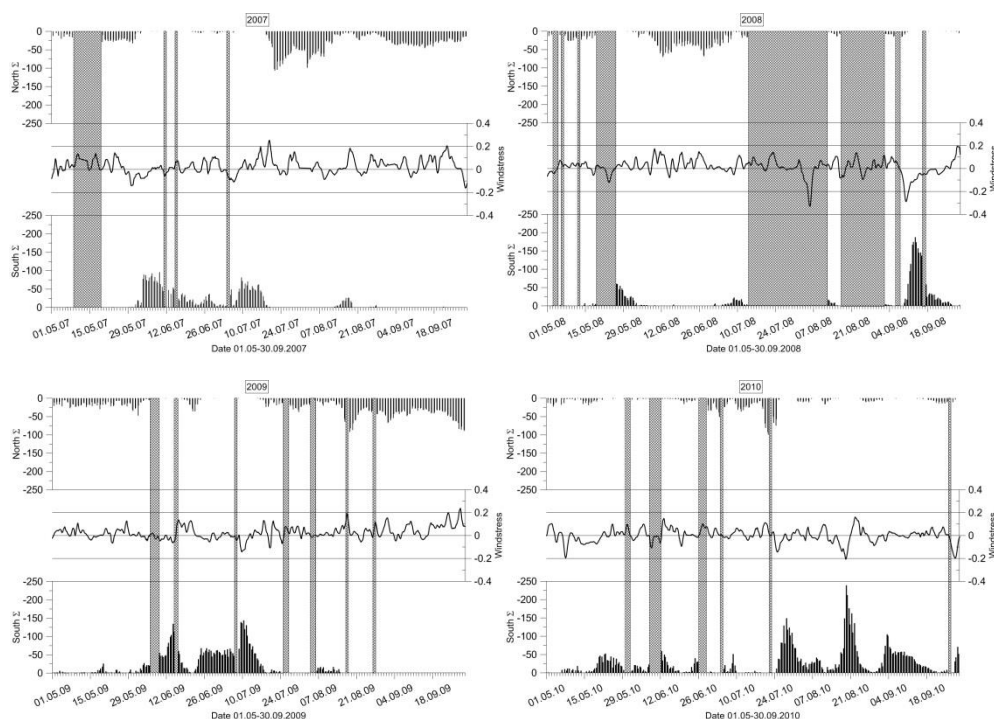
367

368 We selected a criterion to detect whether an upwelling event occurs or not as the value of the
 369 upwelling index (*UI*) exceeded 40 °C (in absolute values while *UI* is by definition a negative
 370 number). The upwelling events found using the selected criterion were also the occasions when
 371 the maximum negative temperature deviation from the transect mean value was at least -2 °C
 372 (except one event on 10-17 September 2007 when the maximum deviation was -1.97 °C).
 373 Furthermore, no other cases with negative temperature deviations exceeding -2 °C were detected.

374 Thus, the criterion $UI < -40\text{ }^{\circ}\text{C}$ gives quite similar results as the criterion based on the maximum
375 negative temperature deviation of $-2\text{ }^{\circ}\text{C}$.

376
377 We identified in May-September 2007-2013 altogether 33 upwelling events, approximately half
378 of them (17) near the northern coast and half (16) near the southern coast (Table 2). The number
379 of days with the upwelling near the northern coast was 150 and near the southern coast 140. As
380 the total number of days with measurements was 838, the upwelling occurred in 18 % and 17 %
381 of days off the northern and southern coast, respectively. The maximum negative temperature
382 deviation from the transect mean value was detected in August 2010 near the southern coast
383 when it reached $-7.78\text{ }^{\circ}\text{C}$. While the maximum temperature deviation characterizes the peak of
384 the upwelling, the introduced cumulative upwelling index also takes into account the extent of
385 the upwelling in space and time. Regarding *CUI* the largest upwelling events were observed in
386 2013 – on 15-30 September 2013 off the southern coast ($CUI = -40.2\text{ }^{\circ}\text{C day}$) and on 11-31
387 August 2013 off the northern coast ($CUI = -39.7\text{ }^{\circ}\text{C day}$). The average *CUI* value of all
388 upwelling events off the northern coast was $-14.5\text{ }^{\circ}\text{C day}$ and off the southern coast $-16.2\text{ }^{\circ}\text{C day}$.
389 The sum of *CUI* values of all detected upwelling events off the northern coast was $-247.0\text{ }^{\circ}\text{C day}$
390 and off the southern coast $-258.4\text{ }^{\circ}\text{C day}$.

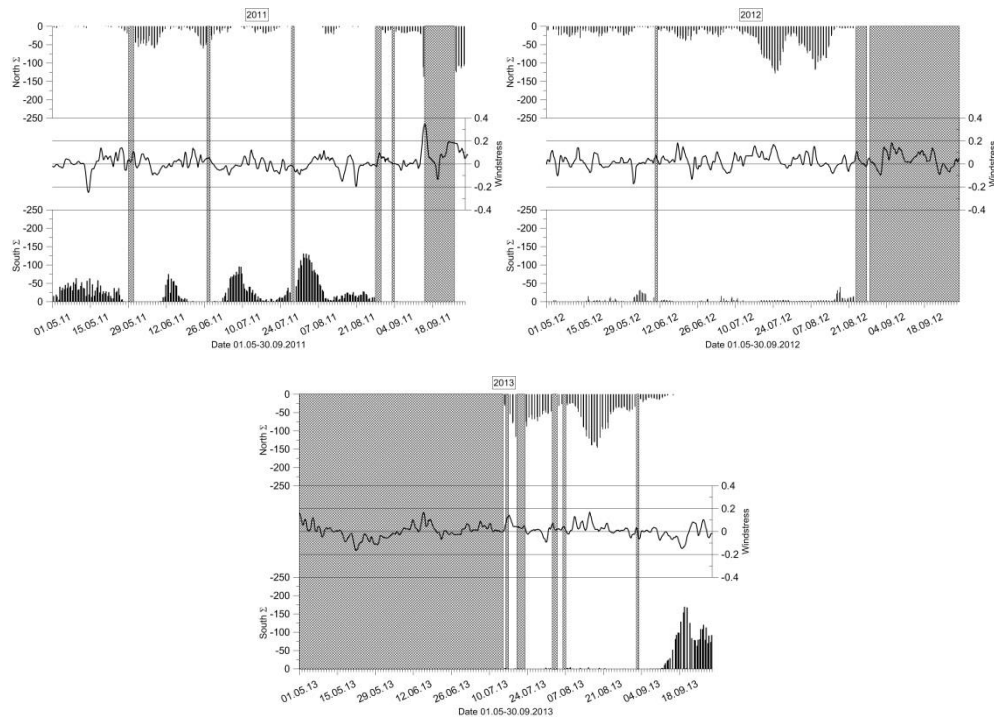
391



392

393

394



395

396

397 **Figure 5. Temporal changes in upwelling index off the northern coast (at the top of each subplot; °C) and off the southern coast at the**
 398 **bottom of each subplot; °C) and along-gulf wind stress (black curve in the middle; N m⁻²) in May-September 2007 (a), 2008 (b), 2009 (c), 2010**
 399 **(d), 2011 (e), 2012 (f) and 2013 (g).**

400

401 The total *CUI* for all measurement days in 2007-2013 was -405.3 °C day for the northern coastal
 402 area and -356.6 °C day for the southern coastal area. Thus, the negative temperature deviations
 403 from the transect mean were more common for the northern coastal sea area while the upwelling
 404 events were more intense in the southern coastal sea area.

405

406 The highest number of upwelling events was observed in July – 10 events, 5 off the northern
 407 coast and 5 off the southern coast, and the lowest in May – 4 events. The sum of *CUI* values of
 408 all events in July and August were -185.3 °C day and -187.9 °C day, respectively, while it was
 409 only -28.6 °C day in May. Obviously, the revealed seasonal trend was partly related to the
 410 temperature difference between the surface layer and the cold layer beneath the seasonal
 411 thermocline, which has its maximum in the Gulf of Finland in July-August (Liblik and Lips,
 412 2011).

413

414 3.3 Upwelling characteristics in relation to wind forcing

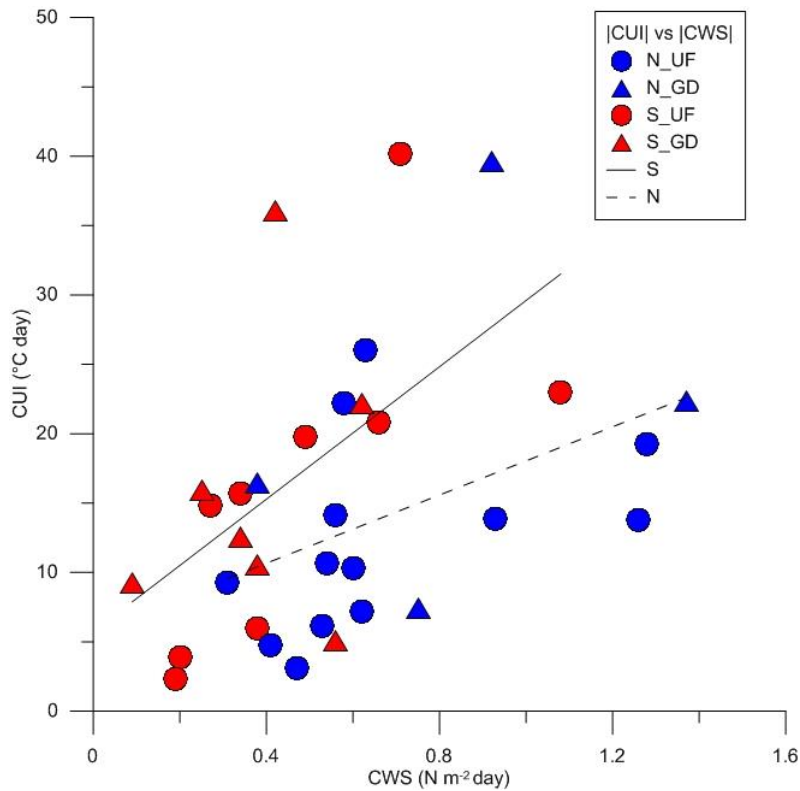
415

416 The occurrence of coastal upwelling events in the Gulf of Finland can be related quite well to the
417 variations of the along-gulf wind stress (Fig. 5). The upwelling events appeared after a certain
418 favorable wind pulses with long enough duration and magnitude. In the case of upwelling events
419 off the northern coast, the positive along-gulf wind stress was usually observed a few days before
420 the event and in the case of upwelling events off the southern coast, the wind stress was negative
421 for a few days (Fig. 5).

422

423 The estimated cumulative wind stress for the detected upwelling events varied between 0.31 and
424 $1.37 \text{ N m}^{-2} \text{ day}$ for westerly winds and between -0.09 and $-1.08 \text{ N m}^{-2} \text{ day}$ for easterly winds
425 (Table 2). The cumulative wind stress associated with each upwelling event was calculated based
426 on daily average wind stress values by summing them up from the first day with favorable wind
427 stress (within a period of 1 week before the event) to the last day with favorable wind stress
428 before the end of the event. If only one day with opposite wind stress appeared in a sequence in
429 the favorable wind stress series, then the calculation period was not broken. The average value of
430 the cumulative wind stress for an upwelling event off the northern coast was $0.71 \text{ N m}^{-2} \text{ day}$ and
431 off the southern coast $-0.44 \text{ N m}^{-2} \text{ day}$. It suggests that to produce a coastal upwelling event of an
432 equal magnitude the required favorable along-gulf wind stress has to be larger for the upwelling
433 events off the northern coast than for the events off the southern coast. This conclusion is drawn
434 by taking into account the above result that the average upwelling intensity (estimated as *CUI*)
435 was similar for the both coastal areas with slightly higher values of *CUI* for the upwelling events
436 off the southern coast. This suggestion is also supported by comparison of relationships between
437 the *CUI* and cumulative wind stress (*CWS*) related to the upwelling events near the opposite
438 coasts (Fig. 6). The linear regression lines between the *CUI* and *CSW* indicate that at the same
439 *CSW* values, the upwelling events had higher intensities off the southern coast than off the
440 northern coast. Nevertheless, the results are quite scattered, and the coefficient of determination
441 (r^2) between the *CUI* and *CSW* are 0.30 for the southern and 0.19 for the northern upwelling
442 events.

443



444

445 **Figure 6. The relationship between the cumulative upwelling index (CUI) and cumulative along-gulf wind stress (CWS) based on 33**
 446 **detected upwelling events in May-September 2007-2013. Red symbols indicate the events off the southern coast and blue symbols the**
 447 **events off the northern coast; circles correspond to the events with pronounced upwelling front (N_UP and C_UP) and triangles the**
 448 **events with a gradual decrease in temperature towards the coast (N_GD and S_GD). The linear regression lines for southern (solid line)**
 449 **and northern upwelling events (dashed line) are shown.**

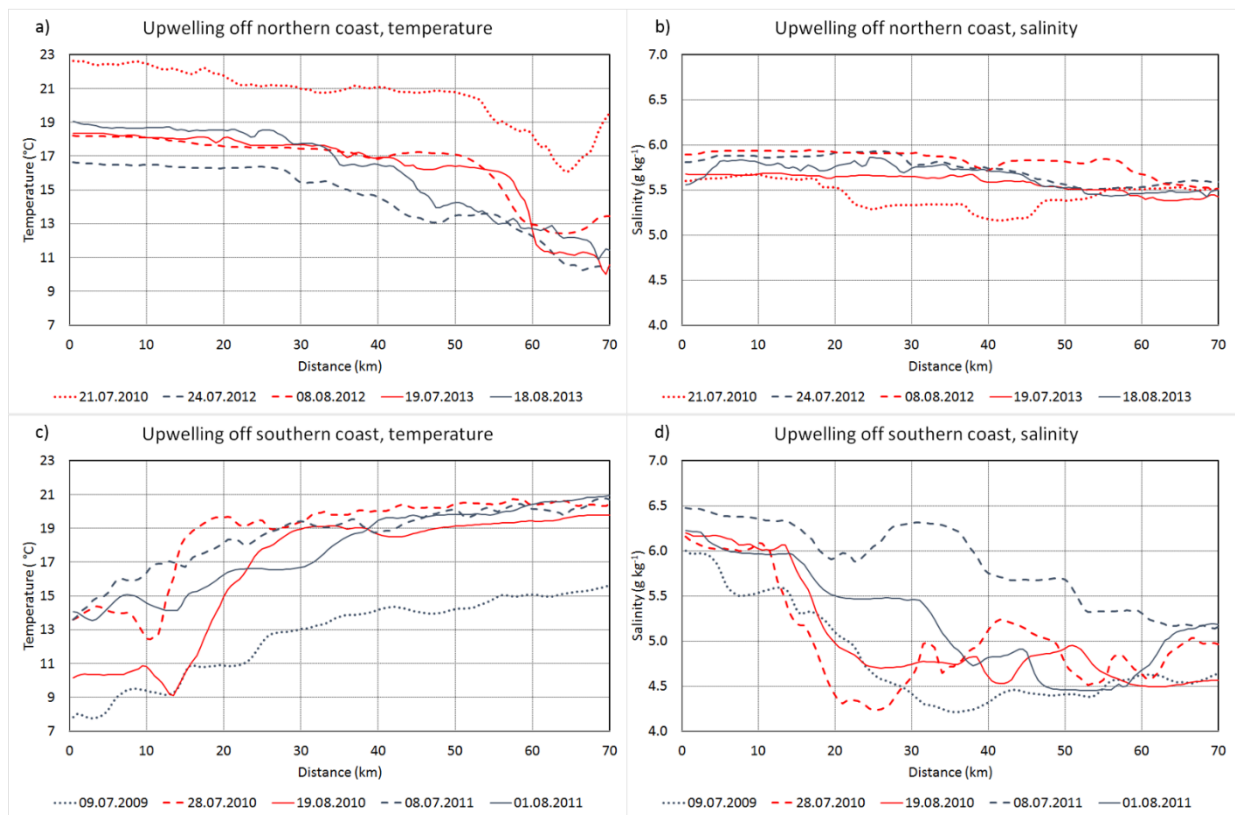
450

451 The average along-gulf wind stress for the entire study period from May to September in 2007-
 452 2013 was 0.016 N m^{-2} . The seasonal averages had positive values in all studied years indicating
 453 that the westerly-south-westerly winds prevailed in the region. The average values of wind stress
 454 varied between 0.001 N m^{-2} in 2010 and 0.029 N m^{-2} in 2007, 2009 and 2012. In May-September
 455 2010, when five upwelling events occurred off the southern coast and only one event off the
 456 northern coast, the average along-gulf wind stress was close to zero indicating that the
 457 cumulative wind forcing was almost equal from both directions. Furthermore, the wind stress
 458 averaged over all observed upwelling events in 2007-2013 was 0.015 N m^{-2} , which is very close
 459 to the average wind stress over the entire study period. This estimate was obtained based on the
 460 mean length of upwelling events of 8.8 days and mean cumulative wind stress values of 0.71 and
 461 $-0.44 \text{ N m}^{-2} \text{ day}$ off the northern and southern coasts, respectively. It can be concluded that the
 462 difference between the wind impulses needed for the generation of upwelling events with similar

463 intensity near the opposite coasts is comparable to the average along-gulf wind stress in the
464 region.

465
466 Usually, the upwelling events occurred one or a few days after the start of the favorable wind
467 pulse, and the maximum of upwelling intensity was reached one or a few days after the
468 maximum wind stress (Fig. 5). We made an attempt to reveal characteristic spatial temperature
469 and salinity distributions in the surface layer from coast to coast at times of the maximum
470 intensity of upwelling events. Surprisingly, the results did not differ significantly between the
471 northern and southern coast – two characteristic shapes of upwelling events in the temperature
472 distribution were identified for both coastal areas.

473



474

475 **Figure 7. Characteristic distributions of temperature and salinity along the ferry route Tallinn-Helsinki with coastal upwelling events off the**
476 **northern coast (a, b) and off the southern coast (c, d); x-axis shows the distance from the Tallinn Bay (latitude 59.48 N) in km along the**
477 **meridional transect.**

478

479 Mostly the upwelling events were characterized by a sharp and very intense temperature front
480 between the upwelling waters and the rest of the transect (red curves in Fig. 7a and c). The sharp

481 upwelling fronts are usually associated with strong along-front jet currents, for instance, as
482 measured by Suursaar and Aps (2007) in the Gulf of Finland in summer 2006. Typical for such
483 events were an almost uniform temperature outside the upwelling area and the temperature
484 minimum (maximum temperature deviation) close to the upwelling front. The other distribution
485 pattern (dark blue curves in Fig. 7a and c) exposed a gradual decrease of temperature towards the
486 upwelling waters. Typical for the latter events were the irregularities in temperature distribution
487 with a characteristic scale of a few kilometers and the temperature minimum (maximum
488 temperature deviation) in the cell closest to the shore. In some cases, e.g. the event near the
489 northern coast with maximum intensity on 18 August 2013 (dark blue solid curve in Fig. 7a), the
490 observed temperature deviations were as large as during the upwelling events with strong
491 temperature front. There was also a third type of temperature distribution when the upwelling
492 waters were not attached to the shore (red dotted curve in Fig. 7a) at least according to the
493 measurements along the ferry route. All these types of upwelling events are well recognized on
494 the maps of temporal changes of temperature and temperature deviation along the ferry route
495 Tallinn-Helsinki (Figs. 2 and 4).

496
497 The spatial distribution of salinity in the surface layer from coast to coast drastically differed
498 between the upwelling events near the northern coast and the events near the southern coast (Fig.
499 7b and d). In the latter case, both the salinity difference across the gulf and the spatial variability
500 at scales of a few to ten kilometers were much larger than in the former case. It is also interesting
501 that in the case of southern upwelling events, the salinity minimum along the transect can be
502 situated either very close to the upwelling front (e.g. on 28 July 2010) or near the northern coast
503 (e.g. 8 July 2011). Although such diverse patterns are partly related to the history of water
504 movements in the gulf, the salinity minimum (at least local minimum) close to the upwelling
505 front might be caused by the westward current jet along the front as also revealed by model
506 experiments (Laanemets et al., 2011). The salinity distribution across the gulf associated with the
507 northern upwelling events is very uniform with some variability at scales of a few to ten
508 kilometers, which have the amplitude several times less than spatial salinity variations associated
509 with the southern upwelling events.

510

511 **4. DISCUSSION**

512

513 Several studies have shown how the Ferrybox measurements are successfully used for different
514 applications, such as for monitoring of coastal waters in combination with remote sensing
515 (Petersen et al., 2008), estimating carbon fluxes and primary productivity (Schneider et al., 2014)
516 and detecting cyanobacterial blooms (Seppälä et al., 2007). However, not enough attention is
517 paid to the Ferrybox systems, especially to the question how the results are affected by the used
518 technical solutions (like water intake depth and construction, piping, etc.). Furthermore, the
519 particularities of geographical location as well as the ferry route and schedule often determine
520 the most suitable applications and requirements for the data treatment. A good example of taking
521 advantage of the geographical location and ferry route is demonstrated by Buijsman and
522 Ridderinkhof (2007) who estimated the water and suspended matter exchange between the
523 Wadden Sea and the North Sea using data collected along the ferry route Den Helder – Texel.

524

525 The ferry route between Tallinn and Helsinki across the elongated Gulf of Finland and the
526 schedule consisting of two cruises a day and a short 1.5-hour stay in Helsinki made it possible to
527 introduce a procedure for correction of coordinates of measurement points and an additional
528 quality check routine for the collected data. The correlation between the data from the two
529 crossings on the same day should be high enough; otherwise, the data can be marked as
530 suspicious. We found that the highest correlation between the two datasets is achieved when the
531 data points are shifted by 3-4 minutes depending on the intake installation and the ferry. This
532 analysis also demonstrates the confidence of the applied Ferrybox system even though the water
533 is taken in through a relatively large sea chest. Furthermore, the ferry route across the relatively
534 narrow gulf from coast to coast is very convenient to collect data on the offshore extension and
535 intensity of coastal upwelling events.

536

537 Various methods have been applied to reveal characteristic features of coastal upwelling events
538 in the Baltic Sea based on data mainly from remote sensing and numerical models. Data of high-
539 resolution long-term Ferrybox measurements have not been analyzed with this aim until now.
540 Certain temperature isoline as the border of the upwelling area was used by Uiboupin and
541 Laanemets (2009) and a temperature deviation (2 °C) from the mean temperature along zonal
542 transects was employed by Lehmann et al. (2012). The latter method is similar to the approach

543 applied in the present study, but we argue that the analysis of temperature deviations along
544 meridional transects is more appropriate in the Gulf of Finland. This conclusion is justified by
545 the fact that, on average, the north-south temperature gradient is negligible in the gulf (see Fig.
546 3a) while the west-east temperature gradient could exist between the shallower and narrower
547 Gulf of Finland and the deeper and wider Northern Baltic Proper due to differential warming and
548 cooling.

549
550 Nevertheless, it is interesting that our results on upwelling frequencies of about 17-18 % near the
551 northern and southern coast are very close to the results of Lehmann et al. (2012) if their results
552 based on remote sensing data were considered. They concluded that upwelling events were
553 present more than 15 % of time near the northern coast and about 15 % of time near the southern
554 coast. At the same time, the estimates of corresponding upwelling frequencies based on
555 numerical experiments differ from the values obtained from the remote sensing data and the
556 results of the present study. Based on model results, the northern coastal area has been suggested
557 as the main upwelling area in the Gulf of Finland with the upwelling occurrence up to 30 % of
558 time (Lehmann et al., 2012; Myrberg and Andrejev, 2003) while near the southern coast
559 downwelling should prevail (Myrberg and Andrejev, 2003).

560
561 Analysis of wind data has also suggested that the coastal upwelling events should occur more
562 often along the northern coast than along the southern coast of the Gulf of Finland (Lehmann et
563 al., 2012; Uiboupin and Laanemets, 2009). The data set consisting of 838 days of measurements
564 from coast to coast used in the present analysis has revealed that, on average, the frequency of
565 upwelling events and their intensity are similar near the northern and southern coast of the gulf
566 although the wind data from the same period suggest prevalence of upwelling events off the
567 northern coast. Partly, this outcome can be explained by the higher position of the thermocline,
568 steeper bottom slope and greater depths in the southern part of the gulf as suggested by some
569 earlier studies (e.g. Väli et al., 2011; Laanemets et al. 2009). Based on a simple theory of
570 upwelling dynamics linking the position of the onshore return flow with the bottom slope and
571 stratification (Lentz and Chapman, 2004), Laanemets et al. (2009) estimated that the onshore
572 return flow should occur in the near-bottom layer for both northern and southern upwelling
573 events in the Gulf of Finland. Due to the steeper slope and greater depths, the upwelling outcome

574 in the vertical transport of cold and nutrient rich waters could be more intense in the southern
575 gulf (Väli et al., 2011; Laanemets et al., 2009).

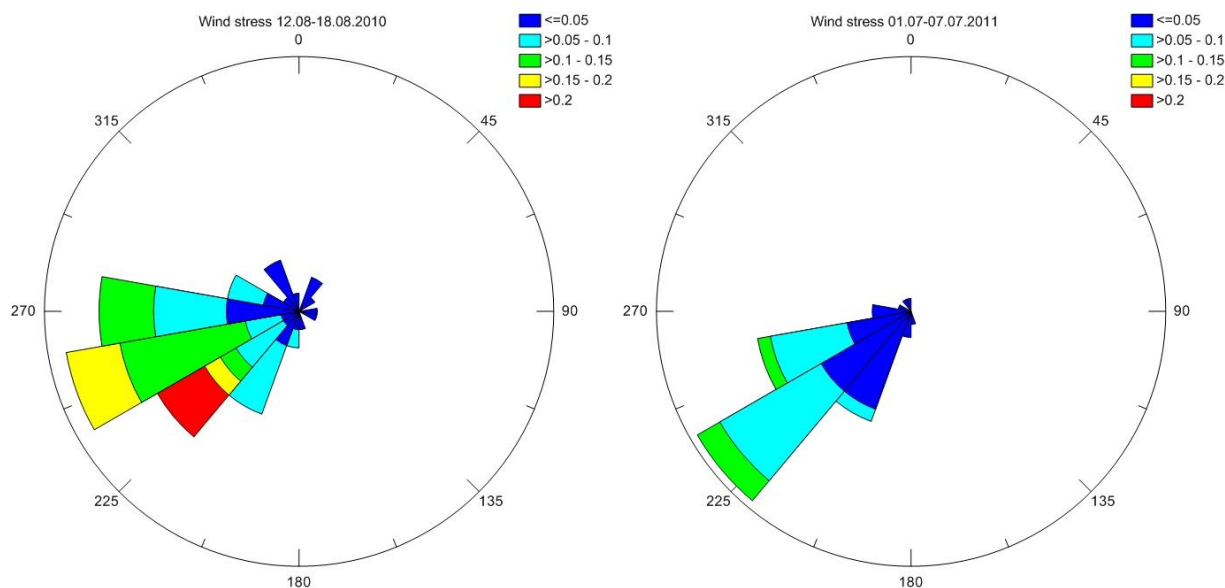
576
577 An additional explanation could be suggested if taking into account the estuarine character of the
578 Gulf of Finland – the basin has free water exchange with the Baltic Proper in the west while it is
579 closed in the east where the main freshwater source is located. First, this basin configuration and
580 the prevalence of southwesterly winds together with the Coriolis force cause a general cyclonic
581 circulation in the surface layer of the gulf (Alenius et al., 1998). Such circulation, in accordance
582 with the geostrophic balance, yields in a higher sea level and deeper thermocline at the northern
583 part of the gulf (e.g. see Andrejev et al., 2004). A similar transverse thermohaline and residual
584 flow structure has been noted by Thomson et al. (2007) in the Juan de Fuca Strait. Liblik and
585 Lips (2016) also concluded that the thermocline is on average at a deeper depth in the northern
586 Gulf of Finland based on their analysis of the data from 35 cross-gulf CTD surveys conducted in
587 2006-2013. Thus, the wind impulse needed for the initiation of a coastal upwelling event near the
588 southern coast can have a smaller magnitude. This suggestion is supported by the comparison of
589 the lowest cumulative wind stress values, which have initiated upwelling events in 2007-2013
590 near the two coasts. The lowest *CWS* value related to an upwelling event along the northern coast
591 is larger than the *CWS* values for five upwelling events along the southern coast (see Fig. 6).

592
593 Secondly, we suggest that for a stronger wind impulse during a longer period, the estuarine
594 character of the basin has a significant influence on the outcome. The strong southwesterly (up-
595 estuary) winds counteract to the estuarine circulation and cause an inflow (convergence) in the
596 surface layer (Elken et al., 2003; Lips et al., 2008b), and thus, a downward movement of the
597 thermocline in the gulf as a whole. In contrary, the down-estuary winds intensify the outflow
598 (cause divergence) in the surface layer, and thus, a general upward movement of the thermocline
599 in the gulf. Consequently, the up-estuary southwesterly winds, on the one hand, cause upwelling
600 along the northern coast, but on the other hand downwelling in the gulf as a whole that could
601 weaken the outcome. In the case of the down-estuary easterly-northeasterly winds, a general
602 upward movement of the thermocline in the gulf supports the coastal upwelling along the
603 southern coast. Such response of the water movements to the forcing could be an explanation
604 why, in general, the cumulative upwelling indexes (presented in Fig. 6) increase faster with the

605 strengthening of the favorable wind stress (CWS in Fig. 6) for the southern upwelling events than
606 for the northern upwelling events.

607
608 The average cross-gulf distributions of temperature and salinity were described based on the 7-
609 year data set of horizontal profiles. On average, the surface layer temperature did not have any
610 horizontal gradient while the surface layer salinity was higher in the southern part than in the
611 northern part of the gulf. The result that the surface water with the lowest salinity was on average
612 at about 20 km from the northern coast supports the suggested general circulation scheme in the
613 Gulf of Finland (e.g. Andrejev et al., 2004). At the same time, if the wind forcing favorable for
614 upwelling events near the southern coast prevailed (as it was observed in summer 2010) the low
615 salinity water appeared in the southern part of the open gulf, close to the upwelling front. This
616 phenomenon was also observed during an intense upwelling event in August 2006 (Lips et al.,
617 2009); it was modeled by Laanemets et al. (2011) and noted by Liblik and Lips (2016) based on
618 an analysis of CTD data from surveys across the gulf in 2006-2013.

619



620
621 **Figure 8. Polar histogram of wind stress vectors ($N m^{-2}$) based on the wind data from a weekly period before the peak of upwelling events off**
622 **the Estonian coast on 17-23 August 2010 (left panel) and 5-11 July 2011 (right panel).**

623
624 The most intense upwelling events regarding temperature deviations were observed near the
625 southern coast as it was also found by Uiboupin and Laanemets (2009, 2015). However, we did

626 not identify clear differences in the temperature distribution patterns between the upwelling
627 events off the two coasts. Instead, near the both coasts, the classical distribution with a sharp
628 temperature front as well as the distribution characterized by a gradual decrease in temperature
629 towards the coast have been observed. We suggest that the upwelling events with the gradual
630 temperature decrease could be associated with the development of upwelling filaments, which
631 occurred under certain conditions and stayed in our measurement window.

632
633 In the case of the upwelling events along the southern coast, the wind speed was on average
634 higher before the events with the sharp temperature front (see Fig. 6 and Table 2). For instance,
635 the polar histograms of wind stress vectors shown in Fig. 8 are very similar except the
636 distribution of wind stress magnitudes. The period before the culmination of the upwelling event
637 with the sharp temperature front observed on 19 August 2010 had a large share of wind stress
638 values $> 0.15 \text{ N m}^{-2}$. Nevertheless, the two prominent upwelling events along the northern coast
639 – the most intense event (on 11-31 August 2013) and the event corresponding to the largest
640 cumulative wind stress (on 18-27 July 2012), were both characterized by the gradual decrease in
641 temperature towards the coast (Fig. 6).

642
643 The filaments of upwelled waters are characteristic features of the upwelling events in the Gulf
644 of Finland (Uiboupin and Laanemets, 2009). Zhurbas et al. (2008) have shown based on a
645 numerical experiment that the cold/warm water squirts and filaments could develop after the
646 weakening of the upwelling favorable winds. Similarly, the squirts and filaments could develop
647 if the wind forcing is strong enough to initiate an upwelling event but not as strong as needed to
648 retain the mesoscale frontal dynamics. In the case of the southern upwelling events, it explains
649 why upwelling events with the gradual decrease of temperature mostly occurred when the wind
650 forcing was on average weaker.

651
652 As shown by Zhurbas et al. (2006), the baroclinic instability of the upwelling jet is expected to
653 occur when the bottom slope is smaller than the isopycnal slope. Thus, for the strong upwelling
654 events, the filaments might appear with a higher probability in the case of northern upwelling
655 events since the bottom slope is about two times shallower in the northern gulf than in the
656 southern gulf (Uiboupin and Laanemets, 2009). The prevailing westerly-southwesterly winds,

657 which cause an inflow in the upper layer and a compensating outflow in the deeper layers (Elken
658 et al., 2003; Liblik and Lips, 2012), could lead to the deepening of the seasonal thermocline in
659 the gulf in 2012 and 2013. The two very intense upwelling events with the gradual temperature
660 decrease were observed in these summers along the northern coast. Since the upwelling
661 dynamics is dependent on the vertical structure of the water column before the event (e.g. Lentz
662 and Chapman, 2004), these suggestions have to be studied further in the future by combining
663 Ferrybox data (restricted to the surface layer and single transect) with the remote sensing and
664 water column data.

665

666 **5. CONCLUSIONS**

667

668 We showed that Ferrybox data from the Tallinn-Helsinki ferry route could be successfully
669 employed to describe the characteristics of coastal upwelling events in the Gulf of Finland. An
670 advantage of the geographical location of the ferry route across the relatively narrow gulf and the
671 schedule consisting of two crossings a day allowed to control the quality of the data and
672 introduce the upwelling index based on the data from a single crossing and the cumulative
673 upwelling index. In total, 33 coastal upwelling events were identified in May-September 2007-
674 2013. It is shown that the upwelling occurrences of 18 % and 17 % of days, as well as intensities
675 of upwelling events, are similar near the northern and southern coast. The most intense events
676 occur in July-August, most probably because of the warmest surface layer (strongest
677 thermocline) during those months. It is shown that the wind impulse needed to generate
678 upwelling events of similar intensity differs between the two coastal areas. We suggest that the
679 general thermohaline structure (adapted to the prevailing forcing) and the estuarine character of
680 the basin are reasons for the found different outcome. The thermohaline structure of the Gulf of
681 Finland is characterized by a deeper position of the thermocline in the northern gulf; thus, the
682 upwelling initiation requires a stronger southwesterly wind impulse to cause upwelling along the
683 northern coast as compared to a weaker northeasterly impulse to cause upwelling along the
684 southern coast. Furthermore, the estuarine character of the basin leads to the weakening of the
685 upwelling created by the westerly (up-estuary) winds and strengthening of the upwelling created
686 by the easterly (down-estuary) winds. Two types of upwelling events were identified – one
687 characterized by a strong temperature (upwelling) front and the other revealing gradual decrease

688 of temperature from the open sea to the coastal area with maximum temperature deviation very
689 close to the shore. We suggest that the spatial variations in temperature with scales of a few
690 kilometers, which were characteristic for the upwelling events with the gradual temperature
691 decrease, could be signs of the meso- and sub-mesoscale features (filaments and squirts)
692 associated with the upwelling dynamics.

693

694 **Acknowledgements**

695

696 We are grateful to Tallink (Estonia) for the possibility to conduct the measurements on board the
697 ferries. We thank our colleagues, especially Inga Lips and Fred Buschmann, for their help in
698 maintaining the Ferrybox system, and Taavi Liblik for his suggestions regarding data processing.
699 This work was supported by institutional research funding IUT19-6 of the Estonian Ministry of
700 Education and Research and by EU Regional Development Foundation, Environmental
701 Conservation and Environmental Technology R&D Programme project VeeOBS (3.2.0802.11-
702 0043).

703

704 **References**

705

- 706 Alenius, P., Myrberg, K., Nekrasov, A. 1998. The physical oceanography of the Gulf of Finland:
707 a review. *Boreal Environ. Res.*, 3, 97–125.
- 708 Andrejev, O., Myrberg, K., Alenius, P., Lundberg, P.A., 2004. Mean circulation and water
709 exchange in the Gulf of Finland - a study based on three-dimensional modeling. *Boreal*
710 *Environ. Res.*, 9(1), 1–16.
- 711 Buijsman, M.C., Ridderinkhof, H., 2007. Long-term ferry-ADCP observations of tidal currents
712 in the Marsdiep inlet. *J. Sea Res.*, 57, 237–256.
- 713 Elken, J., Raudsepp, U., Lips, U., 2003. On the estuarine transport reversal in deep layers of the
714 Gulf of Finland. *J. Sea Res.* 49, 267–274.
- 715 Haapala, J. 1994. Upwelling and its influence on nutrient concentration in the coastal area of the
716 Hanko Peninsula, entrance of the Gulf of Finland. *Est. Coast. Shelf Sci.*, 38(5), 507–521.
- 717 Hardman-Mountford, N. J., Moore, G., Bakker, D. C. E., Watson, A. J., Schuster, U., Barciela,
718 R., Hines, A., Moncoiffe', G., Brown, J., Dye, S., Blackford, J., Somerfield, P. J., Holt,

719 J., Hydes, D. J., and Aiken, J. 2008. An operational monitoring system to provide
720 indicators of CO₂- related variables in the ocean. – *ICES Journal of Marine Science*, 65,
721 1498–1503.

722 Keevallik, S., Soomere, T., 2010. Towards quantifying variations in wind parameters across the
723 Gulf of Finland. *Estonian Journal of Earth Sciences*, 59(4), 288–297.

724 Kononen, K., Kuparinen, J., Mäkela, K., Laanemets, J., Pavelson, J., Nõmmann, S., 1996.
725 Initiation of cyanobacterial blooms in a frontal region at the entrance to the Gulf of
726 Finland, Baltic Sea. *Limnol. Oceanogr.*, 41, 98–112.

727 Laanemets, J., Väli, G., Zhurbas, V., Elken, J., Lips, I., Lips, U., 2011. Simulation of mesoscale
728 structures and nutrient transport during summer upwelling events in the Gulf of Finland
729 in 2006 *Boreal Environ. Res.*, 16A, 15–26.

730 Laanemets, J., Zhurbas, V., Elken, J., Vahtera, E., 2009. Dependence of upwelling-mediated
731 nutrient transport on wind forcing, bottom topography and stratification in the Gulf of
732 Finland: model experiments. *Boreal Environ. Res.*, 14, 213–225.

733 Lehmann, A., Myrberg, K., Höflich, K., 2012. A statistical approach to coastal upwelling based
734 on the analysis of satellite data for 1990–2009. *Oceanologia*, 54, 369–393.

735 Lehmann, A., Myrberg, K., 2008. Upwelling in the Baltic Sea – A review. *J. Marine Syst.*, 74,
736 S3–S12.

737 Lentz, S.J., Chapman, D.C., 2004. The importance of nonlinear cross-shelf momentum flux
738 during wind-driven coastal upwelling. *J. Phys. Oceanogr.*, 34, 2444–2457.

739 Liblik, T., Lips, U., 2016. Variability of pycnoclines in a three-layer, large estuary: the Gulf of
740 Finland. *Boreal Environ. Res.* (in press).

741 Liblik, T., Lips, U., 2012. Variability of synoptic-scale quasi-stationary thermohaline
742 stratification patterns in the Gulf of Finland in summer 2009. *Ocean Sci.*, 8, 603–614.

743 Liblik, T., Lips, U., 2011. Characteristics and variability of the vertical thermohaline structure in
744 the Gulf of Finland in summer. *Boreal Environ. Res.*, 16A, 73–83.

745 Lips, I., Lips, U. 2008. Abiotic factors influencing cyanobacterial bloom development in the
746 Gulf of Finland (Baltic Sea). *Hydrobiologia*, 614, 133–140.

747 Lips, I., Lips, U., Liblik, T. 2009. Consequences of coastal upwelling events on physical and
748 chemical patterns in the central Gulf of Finland (Baltic Sea). *Cont. Shelf Res.* 29, 1836–
749 1847.

750 Lips, U., Lips, I., Kikas, V., Kuvaldina, N., 2008a. Ferrybox measurements: a tool to study
751 meso-scale processes in the Gulf of Finland (Baltic Sea). *US/EU-Baltic Symposium,*
752 *Tallinn, 27-29 May, 2008. IEEE, (IEEE Conference Proceedings), 1 - 6.*

753 Lips, U., Lips, I., Liblik, T., Elken, J., 2008b. Estuarine transport versus vertical movement and
754 mixing of water masses in the Gulf of Finland (Baltic Sea). *US/EU-Baltic Symposium,*
755 *Tallinn, 27-29 May, 2008. IEEE, (IEEE Conference Proceedings), 1 - 8.*

756 Männik, A., Merilain, M., 2007. Verification of different precipitation forecasts during extended
757 winter-season in Estonia. *HIRLAM Newsletter*, No. 52, 65–70.

758 Myrberg, K., Lehmann, A., Raudsepp, U., Szymelfenig, M., Lips, I., Lips, U., Matciak, M.,
759 Kowalewski, M., Krezel, A., Burska, D., Szymanek, L., Ameryk, A., Bielecka, L.,
760 Bradtke, K., Galkowska, A., Gromisz, S., Jedrasik, J., Kaluzny, M., Kozlowski, L.,
761 Krajewska-Soltys, A., Oldakowski, B., Ostrowski, M., Zalewski, M., Andrejev, O.,
762 Suomi, I., Zhurbas, V., Kauppinen, O.-K., Soosaar, E., Laanemets, J., Uiboupin, R.,
763 Talpsepp, L., Golenko, M., Golenko, N., Vahtera, E., 2008. Upwelling events, coastal
764 offshore exchange, links to biogeochemical processes – Highlights from the Baltic Sea
765 Science Congress at Rostock University, Germany, 19-22 March 2007. *Oceanologia*, 50,
766 95-113.

767 Myrberg, K., Andrejev, O. 2003. Main upwelling regions in the Baltic Sea – a statistical analysis
768 based on three-dimensional modeling. *Boreal Environ. Res.*, 8(2), 97-112.

769 Paerl, H.W., Rossignol, K.L., Guajardo, R., Hall, N.S., Joyner, A., Peierls, B.L., Ramus, J.S.
770 2009. FerryMon: Ferry-Based Monitoring and Assessment of Human and Climatically
771 Driven Environmental Change in the Albemarle-Pamlico Sound System. *Environ. Sci.*
772 *Technol.*, 43, 7609–7613

773 Pavelson, J., Laanemets, J., Kononen, K., S. Nõmman, 1997. Quasi-permanent density front at
774 the entrance to the Gulf of Finland: Response to wind forcing. *Cont. Shelf Res.*, 17, 253-
775 265.

776 Petersen, W., 2014. FerryBox systems: State-of-the-art in Europe and future development. *J.*
777 *Marine Syst.*, 140, 4-12.

778 Petersen W., Wehde, H., Krasemann, H., Colijn, F., Schroeder, F., 2008. FerryBox and MERIS –
779 Assessment of coastal and shelf sea ecosystems by combining in situ and remotely sensed
780 data. *Est. Coast. Shelf Sci.*, 77, 296-307.

781 Rantajärvi, E. (Ed.) 2003. Alg@line in 2003: 10 years of innovative plankton monitoring and
782 research and operational information service in the Baltic Sea. *MERI – Report Series of*
783 *the Finnish Institute of Marine Research*, No. 48, 1-36.

784 Schneider, B., Gülzow, W., Sadkowiak, B., Rehder, G., 2014. Detecting sinks and sources of
785 CO₂ and CH₄ by ferrybox-based measurements in the Baltic Sea: Three case studies. *J.*
786 *Marine Syst.*, 140, 13-25.

787 Seppälä, J., Ylöstalo, P., Kaitala, S., Hällfors, S., Raateoja, P., Maunula, P., 2007. Ship-of-
788 opportunity based phycocyanin fluorescence monitoring of the filamentous cyanobacteria
789 bloom dynamics in the Baltic Sea. *Est. Coast. Shelf Sci.*, 73, 489-500.

790 Suursaar, Ü., Aps, R., 2007. Spatio-temporal variations in hydro-physical and -chemical
791 parameters during a major upwelling event off the southern coast of the Gulf of Finland
792 in summer 2006. *Oceanologia*, 49(2), 209-228.

793 Talpsepp, L., Nõges, T., Raid, T., Kõuts, T. 1994. Hydrophysical and hydrobiological processes
794 in the Gulf of Finland in summer 1987 – characterization and relationship. *Cont. Shelf*
795 *Res.*, 14, 749-763.

796 Thomson, R.E., Mihaly, S.F., Kulikov E.A., 2007. Estuarine versus transient flow regimes in
797 Juan de Fuca Strait, *J. Geophys. Res.*, 112, C09022, doi:10.1029/2006JC003925.

798 Uiboupin, R., Laanemets, J., 2009. Upwelling characteristics derived from satellite sea surface
799 temperature data in the Gulf of Finland, Baltic Sea, *Boreal Environ. Res.*, 14 (2), 297-
800 304.

801 Uiboupin, R., Laanemets, J., 2015. Upwelling parameters from bias-corrected composite satellite
802 SST maps in the Gulf of Finland (Baltic Sea). *IEEE Geoscience and Remote Sensing*
803 *Letters*, 12, 592-596.

804 Vahtera, E., Laanemets, J., Pavelson, J., Huttunen, M., Kononen, K., 2005. Effect of upwelling
805 on the pelagic environment and bloom-forming cyanobacteria in the Western Gulf of
806 Finland, Baltic Sea. *J. Marine Syst.*, 58, 67-82.

807 Väli, G., 2011. Numerical experiments on matter transport in the Baltic Sea. PhD thesis, Tallinn
808 Technical University Press.

809 Väli, G., Zhurbas, V., Laanemets, J., Elken, J., 2011. Simulation of nutrient transport from
810 different depths during an upwelling event in the Gulf of Finland. *Oceanologia*, 53, 431-
811 448.

812 Zhurbas, V., Laanemets, J., Vahtera, E., 2008. Modeling of the mesoscale structure of coupled
 813 upwelling/downwelling events and the related inputs of nutrients to the upper mixed layer
 814 in the Gulf of Finland, Baltic Sea. *J. Geophys. Res.*, 113, C05004, doi:
 815 10.1029/2007JC004280.

816 Zhurbas, V.M., Oh, I.S., Park, T., 2006. Formation and decay of a longshore baroclinic jet
 817 associated with transient coastal upwelling and downwelling: a numerical study with
 818 application to the Baltic Sea. *J. Geophys. Res.*, 111, C04014, doi:
 819 10.1029/2005JC003079.

820

821

822

823

824

825 **Table 1.** Periods of measurements along the ferry route Tallinn-Helsinki in 2007-2013, number
 826 of days with measurements and number of days with upwelling events off the northern coast (N)
 827 and off the southern coast (S).

Year	Ferry	Period	Number of days with data	Number of days with upwelling	
				N	S
2007	Galaxy	1 May – 30 September	141	26	21
2008	Galaxy	1 May – 13 July	90	8	11
	Baltic Princess	13 August – 30 September			
2009	Baltic Princess	1 May – 30 September	145	33	30
2010	Baltic Princess	1 May – 30 September	140	5	32
2011	Baltic Princess	1 May – 30 September	135	19	30
2012	Baltic Princess	1 May – 28 August	113	22	0
2013	Silja Europa	15 July – 30 September	74	37	16

828

829

830 **Table 2.** Characteristics of detected upwelling events; dates, coastal area (N – off northern coast;
 831 S – off southern coast), type (UF – with strong upwelling front, GD - - with gradual decrease of
 832 temperature), maximum temperature deviation from the transect mean value, cumulative

833 upwelling index calculated for each event and cumulative along-gulf wind stress calculated for
 834 upwelling favourable winds before and during the upwelling event.

No	Dates	Coast	Type	Maximum temperature deviation (°C)	Cumulative upwelling intensity (°C day)	Cumulative wind stress (N m ⁻² day)
1.	3-14 June 2007	S	UF	-4.12	-19.8	-0.49
2.	8-16 July 2007	S	GD	-3.02	-12.6	-0.34
3.	21-27 July 2007	N	UF	-4.02	-13.9	0.93
4.	29 July – 8 August 2007	N	GD	-3.64	-16.5	0.38
5.	10-17 September 2007 ⁽¹⁾	N	GD	-1.97	-7.5	0.75
6.	26-28 May 2008 ⁽²⁾	S	UF	-2.52	-3.9	-0.20
7.	11-15 June 2008	N	UF	-2.73	-7.2	0.62
8.	27-29 June 2008	N	UF	-2.27	-6.2	0.53
9.	10-17 September 2008	S	UF	-5.42	-23.0	-1.08
10.	9-16 June 2009	S	UF	-4.77	-14.8	-0.27
11.	24 June – 14 July 2009	S	GD	-5.78	-36.1	-0.42
12.	16-22 August 2009	N	UF	-3.20	-10.7	0.54
13.	28 August – 9 September 2009	N	UF	-2.74	-14.1	0.56
14.	17-30 September 2009 ⁽³⁾	N	UF	-3.09	-19.3	1.28
15.	20-24 May 2010	S	GD	-2.21	-5.1	-0.56
16.	12-13 June 2010 ⁽⁴⁾	S	UF	-2.60	-2.3	-0.19
17.	20-24 July 2010	N	UF	-4.70	-9.3	0.31
18.	26 July – 1 August 2010	S	UF	-6.19	-15.7	-0.34
19.	17-23 August 2010	S	UF	-7.78	-20.8	-0.66
20.	2-12 September 2010	S	GD	-5.27	-16.0	-0.25
21.	4-12 May 2011 ⁽⁵⁾	S	GD	-2.22	-9.3	-0.09
22.	31 May – 8 June 2011	N	UF	-2.32	-10.3	0.60
23.	11-15 June 2011	S	UF	-3.12	-6.0	-0.38
24.	24-27 June 2011	N	UF	-2.40	-4.8	0.41
25.	5-10 July 2011	S	GD	-5.05	-10.6	-0.38
26.	29 July – 7 August 2011	S	GD	-4.69	-22.2	-0.62
27.	14 September 2011 ⁽⁶⁾	N	UF	-4.90	-3.1	0.47
28.	26-30 September 2011 ⁽⁷⁾	N	UF	-3.27	-13.8	1.26
29.	18-27 July 2012 ⁽⁸⁾	N	GD	-4.55	-22.4	1.37
30.	2-13 August 2012	N	UF	-4.17	-22.2	0.58
31.	17 July – 1 August 2013 ⁽⁹⁾	N	UF	-6.15	-26.0	0.63
32.	11-31 August 2013	N	GD	-5.03	-39.7	0.92
33.	15-30 September 2013	S	UF	-7.34	-40.2	-0.71

835

836 ⁽¹⁾ temperature deviation was less than -2 °C during the event on 10-17 September 2007

837 ⁽²⁾ data absent before 26 May 2008 for more than 1 day
838 ⁽³⁾ data analysed until 30 September 2009 (upwelling event did further)
839 ⁽⁴⁾ data absent before 12 June 2010 for more than 1 day
840 ⁽⁵⁾ early spring with possible contribution of difference in surface water warming
841 ⁽⁶⁾ no data available after 14 September 2011
842 ⁽⁷⁾ no data available before 26 September 2011, wind data missing on 24-26 September 2011
843 ⁽⁸⁾ wind data on 14-15 July 2012 not available
844 ⁽⁹⁾ ferrybox data on 20-21 July 2013 not available

845
846
847
848

849 **Figure captions**

850

851 **Figure 1.** Map of the Baltic Sea (a) and the study area with the Ferrybox transect and
852 Kalbadagrund meteorological station.

853

854 **Figure 2.** Temporal changes of temperature (in °C) and salinity (in g kg⁻¹) distributions between
855 Tallinn and Helsinki from 1 May to 30 September in 2007 (a, b), 2008 (c, d), 2009, (e, f), 2010
856 (g, h), 2011 (i, j), 2012 (k, l) and 2013 (m, n); y-axis shows the distance from the Tallinn Bay
857 (latitude 59.48 N) in km along the meridional transect.

858

859 **Figure 3.** Distributions of temperature (in °C) and salinity (in g kg⁻¹) deviations from the transect
860 mean value along the ferry route Tallinn-Helsinki for all measurements in May-September 2007-
861 2013 (a, b), 2009 (c, d) and 2010 (e, f). Mean values for each 0.5-km cell (solid curves) and
862 plus/minus RMSE (dashed curves) are shown; x-axis shows the distance from the Tallinn Bay
863 (latitude 59.48 N) in km along the meridional transect.

864

865 **Figure 4.** Temporal changes of spatial distributions of temperature deviations (in °C) from the
866 daily transect mean value between Tallinn and Helsinki from 1 May to 30 September in 2007 (a),
867 2008 (b), 2009, (c), 2010 e), 2011 (f), 2012 (g) and 2013 (h); y-axis shows the distance from the
868 Tallinn Bay (latitude 59.48 N) in km along the meridional transect.

869

870 **Figure 5.** Temporal changes of upwelling index off the northern coast (at the top of each
871 subplot; °C) and off the southern coast (at the bottom of each subplot, °C) and along-gulf wind
872 stress (black curve in the middle; N m^{-2}) in May-September 2007 (a), 2008 (b), 2009 (c), 2010
873 (d), 2011 (e), 2012 (f) and 2013 (g).

874

875 **Figure 6.** Relationship between the cumulative upwelling index (CUI) and cumulative along-
876 gulf wind stress (CWS) based on 33 detected upwelling events in May-September 2007-2013.
877 Red symbols indicate the events off the southern coast and blue symbols the events off the
878 northern coast; circles correspond to the events with pronounced upwelling front (N_UF and
879 C_UF) and triangles the events with gradual decrease of temperature towards the coast (N_GD
880 and S_GD). The linear regression lines for southern (solid line) and northern upwelling events
881 (dashed line) are shown.

882

883 **Figure 7.** Characteristic distributions of temperature and salinity along the ferry route Tallinn-
884 Helsinki with coastal upwelling events off the northern coast (a, b) and off the southern coast (c,
885 d); x-axis shows the distance from the Tallinn Bay (latitude 59.48 N) in km along the meridional
886 transect.

887

888 **Figure 8.** Polar histogram of wind stress vectors (N m^{-2}) based on the wind data from a weekly
889 period before the peak of upwelling events off the Estonian coast on 17-23 August 2010 (left
890 panel) and 5-11 July 2011 (right panel).

891